

Research Article

Products of Sulfide/Selenite Interaction Possess Antioxidant Properties, Scavenge Superoxide-Derived Radicals, React with DNA, and Modulate Blood Pressure and Tension of Isolated Thoracic Aorta

Marian Grman,¹ Anton Misak,¹ Lucia Kurakova,² Vlasta Brezova,³ Sona Cacanyiova ⁴,
Andrea Berenyiova,⁴ Peter Balis ⁴, Lenka Tomasova,¹ Ammar Kharma,¹
Enrique Domínguez-Álvarez,⁵ Miroslav Chovanec ⁶, and Karol Ondrias ¹

¹Institute of Clinical and Translational Research, Biomedical Research Center, Slovak Academy of Sciences, Dubravská cesta 9, 845 05 Bratislava, Slovakia

²Department of Pharmacology and Toxicology, Faculty of Pharmacy, Comenius University, Odbojarov 10, 832 32 Bratislava, Slovakia

³Faculty of Chemical and Food Technology, Slovak University of Technology, Radlinského 9, 812 37 Bratislava, Slovakia

⁴Institute of Normal and Pathological Physiology, Centre of Experimental Medicine, Slovak Academy of Sciences, Dubravská cesta 9, 841 04 Bratislava, Slovakia

⁵Instituto de Química Orgánica General, Consejo Superior de Investigaciones Científicas (IQOG-CSIC), 28006 Madrid, Spain

⁶Cancer Research Institute, Biomedical Research Center, Slovak Academy of Sciences, Dubravská cesta 9, 845 05 Bratislava, Slovakia

Correspondence should be addressed to Miroslav Chovanec; miroslav.chovanec@savba.sk
and Karol Ondrias; karol.ondrias@savba.sk

Received 27 June 2019; Accepted 12 September 2019; Published 25 November 2019

Guest Editor: Kyoung Soo Kim

Copyright © 2019 Marian Grman et al. This is an open access article distributed under the Creative Commons Attribution License, which permits unrestricted use, distribution, and reproduction in any medium, provided the original work is properly cited.

Selenium (Se), an essential trace element, and hydrogen sulfide (H₂S), an endogenously produced signalling molecule, affect many physiological and pathological processes. However, the biological effects of their mutual interaction have not yet been investigated. Herein, we have studied the biological and antioxidant effects of the products of the H₂S (Na₂S)/selenite (Na₂SeO₃) interaction. As detected by the UV-VIS and EPR spectroscopy, the product(s) of the H₂S-Na₂SeO₃ and H₂S-SeCl₄ interaction scavenged superoxide-derived radicals and reduced [•]cPTIO radical depending on the molar ratio and the preincubation time of the applied interaction mixture. The results confirmed that the transient species are formed rapidly during the interaction and exhibit a noteworthy biological activity. In contrast to H₂S or selenite acting on their own, the H₂S/selenite mixture cleaved DNA in a bell-shaped manner. Interestingly, selenite protected DNA from the cleavage induced by the products of H₂S/H₂O₂ interaction. The relaxation effect of H₂S on isolated thoracic aorta was eliminated when the H₂S/selenite mixture was applied. The mixture inhibited the H₂S biphasic effect on rat systolic and pulse blood pressure. The results point to the antioxidant properties of products of the H₂S/selenite interaction and their effect to react with DNA and influence cardiovascular homeostasis. The effects of the products may contribute to explain some of the biological effects of H₂S and/or selenite, and they may imply that a suitable H₂S/selenite supplement might have a beneficial effect in pathological conditions arisen, e.g., from oxidative stress.

1. Introduction

Exogenously added and endogenously produced H₂S affects many physiological and pathological processes [1–3]. Accumulating evidence supports the involvement of H₂S in the regulation of cardiovascular homeostasis [4]. It has mostly beneficial effects during oxidative stress by reacting with reactive oxygen and nitrogen species, i.e., hydrogen peroxide (H₂O₂), superoxide anion radical (O₂^{•-}), hypochlorite (HOCl), or peroxyxynitrite (ONOO⁻) [5–8]. However, several effects of H₂S on cells are toxic [9–11].

Selenium (Se) is a relatively rare but an essential trace element for humans, plants, and microorganisms. Se, which exerts multiple and complex effects on human health, is known as an antioxidant due to its presence in 25 selenoproteins in the form of selenocysteine amino acid. Both beneficial and detrimental effects of Se deficiency and/or supplementation are well known. The biological effects of Se compounds (selenite, selenate, selenocysteine, and selenomethionine) on cardiac oxidative damage, heart disease, cancer prevention, immunity, diabetes, neuroregeneration, or dementia have been reported [12–17]. However, the beneficial effect of Se supplementation for men's health is still a controversial issue [18–23]. Selenite, which is a common Se supplement, is considered as a promising anticarcinogen [24–26]. It can induce apoptosis in cancer cells through the production of reactive oxygen species (ROS) leading to oxidative stress [27, 28]. However, Se compounds were also found to damage DNA in healthy cells [29] and therefore may not be considered as a suitable protective agent against cancer and/or other chronic diseases. Actually, they can cause or advance some kinds of cancers [30, 31]. The exact mechanisms of the beneficial and toxic effects of Se are not yet fully understood, giving rise to further uncertainty about its potential use in nutrition supplements and/or clinical treatment.

Se and H₂S are present in living organisms, and each one has beneficial and/or toxic effects through its interaction mostly with ROS [1, 2, 30–33]. However, the biological effects of products of the H₂S/selenite interaction are not yet known, namely, their involvement in the production and/or inhibition of ROS, reaction with DNA, or influence on cardiovascular system. Therefore, we have studied the effects of products of the H₂S/selenite interaction on O₂^{•-} and [•]cPTIO radicals, DNA cleavage, tension of isolated aortic rings, and rat blood pressure (BP). We found that the products have significant biological effects that differ from those caused by H₂S or by selenite on their own. These results may contribute to the understanding of possible coupled biological effects of H₂S and Se.

2. Material and Methods

2.1. Chemicals

2.1.1. Selenium Compounds. Stock solutions of sodium selenite (Na₂SeO₃, 10 or 40 mmol L⁻¹, Merck K34993707-542 or Sigma 214485), selenium tetrachloride (SeCl₄, 10 mmol L⁻¹, Aldrich 323527), and sodium selenate (Na₂SeO₄,

10 mmol L⁻¹, Sigma S0882) were prepared freshly in deionized H₂O, stored at 23°C, and used within 5 h. Na₂SeO₃ dissociates in solution to yield mostly H₂SeO₃ at acidic pH, HSeO₃⁻ at neutral pH, and SeO₃²⁻ at alkaline pH. For simplicity, the term SeO₃²⁻ is employed as representative expression to encompass the total mixture of these different (de)protonation states.

2.1.2. Hydrogen Peroxide. Hydrogen peroxide (H₂O₂) (14.7 mol L⁻¹; Sigma-Aldrich 85321), according to a particular experiment, was diluted in H₂O or in 100 mmol L⁻¹ sodium phosphate buffer, supplemented with 200 or 50 μmol L⁻¹ DTPA, pH 7.4, 37°C before application.

2.1.3. Radicals. 5-*tert*-butoxycarbonyl-5-methyl-1-pyrroline-*N*-oxide (BMPO, 100 mmol L⁻¹, Dojindo B568-10, Japan) was dissolved in deionized H₂O, stored at -80°C, and used after thawing. 2-(4-Carboxyphenyl)-4,4,5,5-tetramethylimidazole-1-oxyl-3-oxide ([•]cPTIO, 10 mmol L⁻¹, Cayman 81540 or Sigma C221) was dissolved in deionized H₂O and was stored at -20°C for several weeks.

2.1.4. Sulfide. Na₂S (100 mmol L⁻¹ stock solution, Dojindo SB01, Japan) was dissolved in argon degassed deionized H₂O, stored at -80°C, and used immediately after thawing. Na₂S dissociates in aqueous solution and reacts with H⁺ to yield H₂S, HS⁻, and a trace of S²⁻. We use the term H₂S to describe the total mixture of H₂S, HS⁻, and S²⁻ forms. The stock concentration was checked by UV-VIS spectroscopy: by the absorbance of 1000x diluted stock solution at 230 nm ($\epsilon_{230\text{nm}} = 7700 \text{ mol}^{-1} \text{ L cm}^{-1}$, diluted by deionized water) and also by the reduction of 100 μmol L⁻¹ DTNB by 2000x diluted stock solution (1 H₂S molecule generates 2 TNB⁻ equivalents, $\epsilon_{412\text{nm}} = 14,100 \text{ mol}^{-1} \text{ L cm}^{-1}$, measured in 1 mmol L⁻¹ phosphate buffer), according to Nagy et al. [34].

2.1.5. Buffers. 100 mmol L⁻¹ sodium phosphate buffer supplemented with 100 μmol L⁻¹ diethylenetriaminepentaacetic acid (DTPA), pH 6.5, 7.0, 7.4, 8.0, and 9.0, 37°C, was employed for UV-VIS experiments. 50 and 25 mmol L⁻¹ sodium phosphate buffer, supplemented with 100 and 50 μmol L⁻¹ DTPA, pH 7.4, 37°C, was used for electron paramagnetic resonance (EPR) and plasmid DNA (pDNA) cleavage studies, respectively.

2.2. UV-VIS of [•]cPTIO. To obtain 1 mL of the working solution, 10 or 100 μL of stock solution of the compounds studied was added to the appropriate volume (990 or 900 μL, respectively) of 100 mmol L⁻¹ sodium phosphate buffer (at given pH, 37°C) containing the final concentrations of 100 μmol L⁻¹ [•]cPTIO and 100 μmol L⁻¹ DTPA. UV-VIS absorption spectra (900–190 nm) were recorded every 30 s for 20 to 40 min with a Shimadzu 1800 (Kyoto, Japan) spectrometer at 37°C. The [•]cPTIO extinction coefficient of 920 mol⁻¹ L cm⁻¹ at 560 nm was used. The reduction of the [•]cPTIO radical was determined as the decrease of the absorbance at 560 nm (absorption maximum of [•]cPTIO in VIS range) or at 358 nm after subtracting the absorbances at 730 or at 420 nm, respectively [5, 35].

To study the involvement of O_2 in the H_2S/SeO_3^{2-} -induced reduction of the $\cdot cPTIO$ radical, 10 mmolL^{-1} Na_2S in H_2O , 10 mmolL^{-1} Na_2SeO_3 in H_2O , and $102\ \mu\text{molL}^{-1}$ $\cdot cPTIO$ in the 100 mmolL^{-1} sodium phosphate buffer, supplemented with $100\ \mu\text{molL}^{-1}$ DTPA (pH 7.4; 37°C), were deaerated with argon for 10 min at 37°C . The compounds were mixed in a closed UV-cuvette, and the UV-VIS spectra were recorded. The O_2 concentration in the deaerated samples was 3-5%, confirmed with an oxygen electrode (OXELP, SYS-ISO2, WPI, USA). In all UV-VIS experiments, H_2O was used as a blank.

2.3. EPR of the \cdot BMPO Adducts. To study the ability of H_2S/SeO_3^{2-} to scavenge the $O_2^{\cdot-}$ radical or its derivatives produced in DMSO/ KO_2 solution, sample preparation and EPR measurements were conducted in accordance with previously reported protocols [5]. The solution (final concentrations) of BMPO (20 mmolL^{-1}), DTPA ($100\ \mu\text{molL}^{-1}$) in sodium phosphate buffer (50 mmolL^{-1} , pH 7.4) was incubated for 1 min at 37°C ; an aliquot of the compound was added, followed by saturated KO_2 /DMSO solution (10% v/v DMSO/final buffer) 3 s later. The sample was mixed for 5 s and transferred to a standard cavity aqueous EPR flat cell. The first EPR spectrum was recorded 2 min after the addition of KO_2 /DMSO solution at 37°C . The sets of individual EPR spectra of the \cdot BMPO spin adducts were recorded as 15 sequential scans, each 42 s, with a total time of 11 min. Each experiment was repeated at least twice. EPR spectra of the \cdot BMPO spin adducts were measured on a Bruker EMX spectrometer, X-band $\sim 9.4\text{ GHz}$, 335.15 mT central field, 8 mT scan range, 20 mW microwave power, 0.1 or 0.15 mT modulation amplitude, 42 s sweep time, 20.48 ms time constant, and 20.48 ms conversion time at 37°C . Intensities of the \cdot BMPO adducts in the EPR spectra were reproducible, when the KO_2 /DMSO stock solution was stored at 5°C for 1 day or at $23 \pm 1^\circ\text{C}$ for 4 h.

2.4. Plasmid DNA Cleavage. pDNA cleavage assay with the use of pBR322 plasmid (New England BioLabs Inc., N3033L) was performed as reported previously [5, 36]. In this assay, all samples contained $0.2\ \mu\text{g}$ pDNA in sodium phosphate buffer (25 mmolL^{-1} sodium phosphate, $50\ \mu\text{molL}^{-1}$ DTPA, pH 7.4, 37°C). After addition of compounds, the resulting mixtures were incubated for 30 min at 37°C . All concentrations listed in the section were final in the samples. After incubation, the reaction mixtures were subjected to 0.6% agarose gel electrophoresis. Samples were electrophoresed in TBE buffer (89 mmolL^{-1} Tris, 89 mmolL^{-1} boric acid, and 2 mmolL^{-1} EDTA) at 5.5 V cm^{-1} for 2 h; gels were stained with GelRedTM Nucleic Acid Gel Stain and photographed using a UV transilluminator. Integrated densities of all pBR322 forms in each lane were quantified using the TotalLab TL100 image analysis software to estimate pDNA cleavage efficiency (Nonlinear Dynamic Ltd., USA).

2.5. Guide for the Use and Care of Laboratory Animals

2.5.1. Isolated Thoracic Aorta. Procedures were performed in accordance with the Institutional Guidelines of the Eth-

ical Committee on the Ethics of Procedures in Animal, Clinical and other Biomedical Experiments (permit number: EC/CEM/2017/4) of the Institute of Normal and Pathological Physiology, Centre of Experimental Medicine and were approved by the State Veterinary and Food Administration of the Slovak Republic and by an Ethical Committee according to the European Convention for the Protection of Vertebrate Animals used for Experimental and other Scientific Purposes, Directive 2010/63/EU of the European Parliament. The Institute of Normal and Pathological Physiology provided veterinary care.

2.5.2. Rat Blood Pressure. All procedures were approved by the State Veterinary and Food Administration of the Slovak Republic (No.: Ro-1545/15-221) according to the guidelines from Directive 2010/63/EU of the European Parliament. Experiments were carried out according to the guidelines laid down by the animal welfare committee of the Institute of Normal and Pathological Physiology of the Slovak Academy of Sciences and conformed to the principles and regulations, as described in the editorial by Grundy [37].

2.6. Functional Study of Isolated Thoracic Aorta. Normotensive Wistar Kyoto (WKY) rats ($307 \pm 4.3\text{ g}$) were killed by decapitation after a brief anesthetization with CO_2 , and the thoracic aorta was isolated as described in our previous study [38]. The changes in isometric tension were measured by the electromechanical transducers (FSG-01, MDE, Budapest, Hungary). The resting tension of 1 g was applied to each ring and maintained throughout a 45 to 60 min of equilibration period until stress relaxation no longer occurred. Changes in thoracic aorta tension were followed by noradrenaline (NA; $1\ \mu\text{molL}^{-1}$) precontracted arterial rings after a stable plateau was achieved.

2.7. Functional Study of Rat Blood Pressure. Male Wistar rats ($n = 10$; $350 \pm 40\text{ g}$) were from the Department of Toxicology and Laboratory Animal Breeding at Dobra Voda, Slovak Academy of Sciences, Slovakia. The rats were housed under a 12 h light-12 h dark cycle, at a constant humidity (45-65%) and temperature ($20\text{-}22^\circ\text{C}$), with free access to standard laboratory rat chow and drinking water. The *Institute of Experimental Pharmacology and Toxicology*, Centre of Experimental Medicine, Slovak Academy of Sciences, provided veterinary care. The tranquilizer xylazine (Rometar) was purchased from Zentiva (Czech Republic), and the anesthetic combination of tiletamine+zolazepam (Zoletil 100) was acquired from Virbac (France). All other chemicals were purchased from Sigma-Aldrich. Experiments were carried out as previously described [39]. Rats were anesthetized with Zoletil 100 (tiletamine+zolazepam, 80 mg kg^{-1} , i.p.) and Rometar (xylazine, 5 mg kg^{-1} , i.p.). During the anesthesia, BP, heart rate, and reflex responses to mechanical stimuli were monitored. The animals were under anesthesia during the whole experiment and were euthanized with an overdose of Zoletil *via* jugular vein at the end of the surgical procedure. All experiments were supervised and performed under the same experimental conditions.

2.8. Blood Pressure Measurement. The right jugular vein was cannulated to administer compounds under anesthesia as described above. The left arteria carotis communis was cannulated for inserting the fiber optic microcatheter pressure transducers (FISO LS 2F Harvard Apparatus, USA). The analog signal was digitalized at 10 kHz, filtered at 1 kHz, and recorded by DEWEsoft 6.6.7 (GmbH, Austria). The signal was evaluated 5 s before and 10 min after compound administration. After stabilization of BP (10–20 min), the compounds were administered into the right jugular vein as a bolus of 500 $\mu\text{L kg}^{-1}$ over 15 s period. The solution of the $\text{H}_2\text{S}/\text{SeO}_3^{2-}$ mixture (10/5 in mmol L^{-1}) was prepared as follows: to 123.5 μL of 100 mmol L^{-1} phosphate buffer, 100 $\mu\text{mol L}^{-1}$ DTPA, 14 μL of 1 mol L^{-1} HCl was added, followed by 62.5 μL of 40 mmol L^{-1} Na_2SeO_3 in 0.9% NaCl, and finally 50 μL of 100 mmol L^{-1} Na_2S in H_2O was added. The pH of the buffered mixture was 7.4. The mixture was incubated for 40 ± 10 s at 23°C before i.v. administration. Unbuffered $\text{H}_2\text{S}/\text{SeO}_3^{2-}$ mixture (10/5 in mmol L^{-1}) was prepared, when 0.9% NaCl was used instead of phosphate buffer and HCl. The pH of the unbuffered mixture was ~ 11 measured by a pH paper indicator.

2.9. Statistical Analysis. Unless otherwise stated, data are represented as the means \pm S.E.M. Statistical significance was determined by Student's *t*-test or one-way ANOVA followed by the multiple comparison test. Differences between means were considered significant at $*P \leq 0.05$. Data analysis and plot construction were carried out using SigmaPlot 12 (Systat Software GmbH).

3. Results

3.1. H_2S Interacts with Na_2SeO_3 and SeCl_4 , but Not with Na_2SeO_4 , to Form Initial Reactive Intermediate(s), which Reduce the $\cdot\text{cPTIO}$ Radical. Since the antioxidant properties of $\text{H}_2\text{S}/\text{SeO}_3^{2-}$ products are unknown, we have used the $\cdot\text{cPTIO}$ radical to study the reducing properties of the products of $\text{H}_2\text{S}/\text{SeO}_3^{2-}$ interaction. The $\cdot\text{cPTIO}$ radical is stable in aqueous solution, and its formation and reduction can be monitored by the UV-VIS spectrophotometry at 358 or 560 nm. Even in the presence of up to 100 $\mu\text{mol L}^{-1}$ H_2S or 100–400 $\mu\text{mol L}^{-1}$ SeO_3^{2-} , the absorbance (ABS) of the radical at 358 and 560 nm decreases only by $<7\%$ after 40 min, indicating that neither H_2S nor SeO_3^{2-} on its own reduces this radical (Figure 1). In contrast, once H_2S (25–100 $\mu\text{mol L}^{-1}$) was added to the $\cdot\text{cPTIO}/\text{SeO}_3^{2-}$ (100/2.5–400 $\mu\text{mol L}^{-1}$) mixture, or SeO_3^{2-} was added to $\cdot\text{cPTIO}/\text{H}_2\text{S}$, the absorbances at 358 and 560 nm decreased rapidly over the time (≤ 30 s), indicating a possible formation of strong reducing agent(s) which fastly and efficiently reduced the $\cdot\text{cPTIO}$ radical (Figures 1 and 2). Similar results were obtained when SeCl_4 , but not Na_2SeO_4 , was used instead of SeO_3^{2-} (Figures S1 and S2a).

The reduction of $\cdot\text{cPTIO}$ followed a bell-shaped dependence on the concentration of SeO_3^{2-} at a constant $\cdot\text{cPTIO}/\text{H}_2\text{S}$ concentration (Figure 2(a)), with a maximum radical scavenging activity at an $\text{H}_2\text{S}:\text{SeO}_3^{2-}$ ratio of roughly 4:1. The ability of H_2S to reduce $\cdot\text{cPTIO}$ in the presence of

SeO_3^{2-} increased with the increasing H_2S concentration (Figure 2(b)) and followed also a bell-shaped dependence on pH (Figures 3 and S3).

If H_2S and SeO_3^{2-} were preincubated for different periods of time before the addition to $\cdot\text{cPTIO}$, it clearly resulted in the highest radical scavenging activity, which was subsequently lost over the time (Figure 4). An $\text{H}_2\text{S}/\text{SeO}_3^{2-}$ (100/100 in $\mu\text{mol L}^{-1}$) mixture preincubated for ≥ 1 min prior to $\cdot\text{cPTIO}$ addition did not reduce $\cdot\text{cPTIO}$, demonstrating that later products of the reaction of sulfide with SeO_3^{2-} could not be responsible for the reduction of the radical and that the relevant active species were formed swiftly, in less than 1 min and have a short lifetime, as recently suggested [40]. Notably, formation of these active early intermediates to reduce $\cdot\text{cPTIO}$ was prolonged with the increase of the $\text{H}_2\text{S}/\text{SeO}_3^{2-}$ ratio (Figure 4(e)). At $\text{H}_2\text{S}/\text{SeO}_3^{2-}$ concentration of 100/25 in $\mu\text{mol L}^{-1}$ and 5 min preincubation time, the mixture still possessed around 50% potency to reduce $\cdot\text{cPTIO}$ (Figure 4(e)). This timing, once more, accounts for a rapidly formed selenosulfide intermediate as being the ultimate responsible for this radical scavenging activity, a species also possibly being sensitive to oxidation over prolonged time periods (Figure 4).

While the available evidence is in accordance with the formation of HSSeSH as the main reactive species, there are other chalcogen-based candidates which are good reducing agents, namely, hydrogen selenide (H_2Se), hydroselenide anion (HSe^-), selenide (Se^{2-}), persulfides, and polysulfides (S_x^{2-}) [41–43]. Interestingly, O_2 does not seem to play a major role in the $\text{H}_2\text{S}/\text{SeO}_3^{2-}$ -induced reduction of the $\cdot\text{cPTIO}$ radical probably due to slower kinetics of interaction of reactants and/or intermediates with O_2 in comparison to the rate of $\cdot\text{cPTIO}$ reduction [44–48]. Under argon flushed conditions, reduction of the $\cdot\text{cPTIO}$ radical was neither enhanced nor suppressed significantly, hence ruling out any major involvement of H_2Se , as this selenium compound is highly sensitive to O_2 (Figure S2b).

3.2. EPR of $\cdot\text{BMPO-OOH}$: The Initial Products of the $\text{H}_2\text{S}/\text{SeO}_3^{2-}$ Interaction Also Scavenge Derivatives of Superoxide Anion ($\text{O}_2^{\cdot-}$) Radical. We aimed to ascertain whether the initial products of the $\text{H}_2\text{S}/\text{SeO}_3^{2-}$ interaction are able to scavenge other radicals, i.e., $\text{O}_2^{\cdot-}$ or its derivatives. The interactions with $\text{O}_2^{\cdot-}$ were studied with the EPR spin trap method based on the reaction of this dioxygen radical with BMPO to form the $\cdot\text{BMPO-OOH}$ adduct [49]. This assay was chosen due to biological and mechanistical reason; $\text{O}_2^{\cdot-}$ is a simple radical reduced by one-electron transfer.

$\text{O}_2^{\cdot-}$ was dissolved in phosphate buffer (pH 7.4, 37°C) and trapped by BMPO. Under these conditions, the relative intensity of the $\cdot\text{BMPO-OOH}$ adduct decreased slowly over the time and was comparable to the values reported under physiological conditions (Figures 5(a1)–5(a3)) [49]. The addition of SeO_3^{2-} (25 and 50 $\mu\text{mol L}^{-1}$) did not significantly interfere with the $\cdot\text{BMPO-OOH}$ adduct formation, its concentration, and rate of decay (Figures 5(b1)–5(b3), S4b1–b3). In contrast, H_2S (25 and 50 $\mu\text{mol L}^{-1}$) decreased the $\cdot\text{BMPO-OOH}$ concentration and increased the rate of the decay, and this “antioxidant” activity of H_2S was

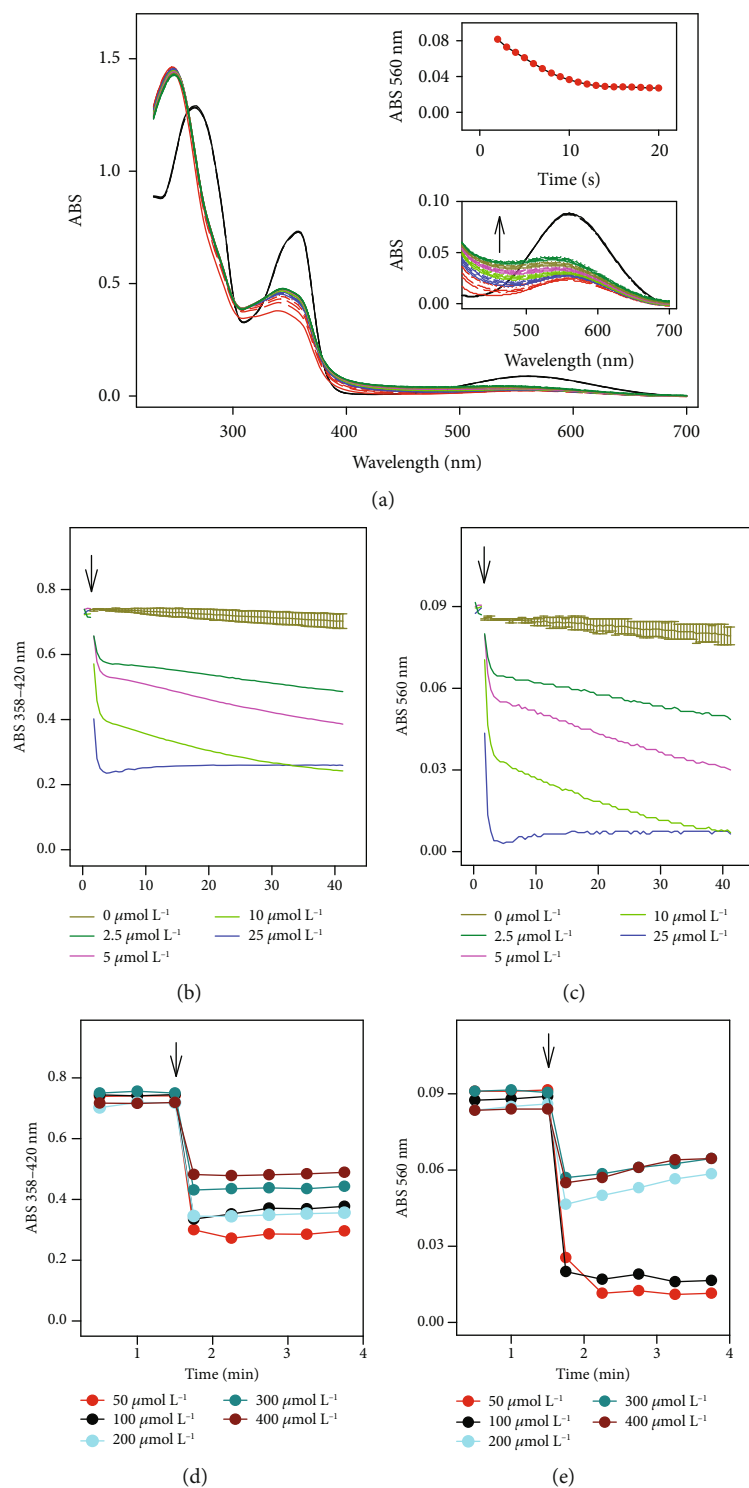


FIGURE 1: Interaction of \cdot cPTIO/ SeO_3^{2-} with H_2S . (a) Time resolved UV-VIS spectra of the interaction of $100 \mu\text{mol L}^{-1}$ \cdot cPTIO with $100 \mu\text{M}$ SeO_3^{2-} (3 times repeated every 30 s, black) and subsequent addition of $100 \mu\text{mol L}^{-1}$ H_2S . Spectra were collected every 30 s for 15 min; the first spectrum, indicated by the solid red line, was measured 15 s after addition of H_2S . Top inset: kinetics of changes in absorbance at 560 nm after addition of $100 \mu\text{mol L}^{-1}$ H_2S into \cdot cPTIO/ SeO_3^{2-} ($100/100$ in $\mu\text{mol L}^{-1}$) solution at time 0 s. Bottom inset: details of the time resolved spectra of the \cdot cPTIO/ SeO_3^{2-} ($100/100$ in $\mu\text{mol L}^{-1}$) interaction before (black) and after addition of H_2S ($100 \mu\text{mol L}^{-1}$, the first spectrum is indicated by the solid red line, which is followed each 30 s by: long dash red, medium dash red, short dash red, dotted red, solid blue line, long dash blue, medium dash blue, etc.). (b, c, d, e) H_2S ($100 \mu\text{mol L}^{-1}$) was added to $100 \mu\text{mol L}^{-1}$ solution of \cdot cPTIO containing different concentrations of SeO_3^{2-} (0 - $400 \mu\text{mol L}^{-1}$, see legend). The kinetics of the reduction of $100 \mu\text{mol L}^{-1}$ \cdot cPTIO before and after addition of $100 \mu\text{mol L}^{-1}$ H_2S (marked by arrow) was monitored as a decrease of the absorbance at 358 nm minus the absorbance at 420 nm (b, d) and also as a decrease of the absorbance at 560 nm (c, e).

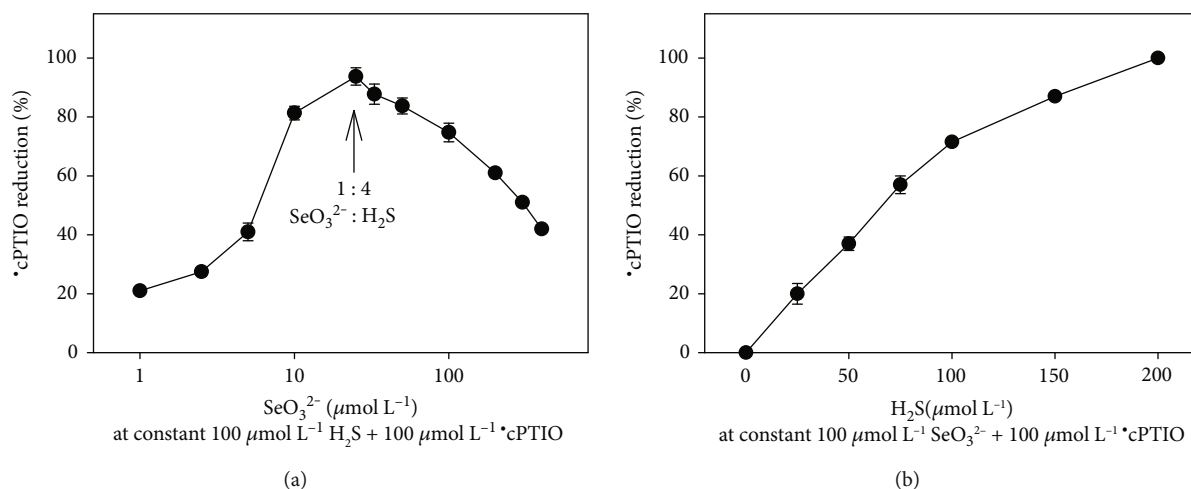


FIGURE 2: Effect of the SeO_3^{2-} and H_2S concentration on the reduction of $\cdot\text{cPTIO}$. (a) Effect of the SeO_3^{2-} concentration ($1\text{--}400\ \mu\text{mol L}^{-1}$) on the reduction of $\cdot\text{cPTIO}$ ($100\ \mu\text{mol L}^{-1}$) in the presence of H_2S ($100\ \mu\text{mol L}^{-1}$). Arrow indicates the $1:4$ molar ratio of $\text{SeO}_3^{2-}:\text{H}_2\text{S}$. (b) Effect of the H_2S concentration ($0\text{--}200\ \mu\text{mol L}^{-1}$) on the reduction of $\cdot\text{cPTIO}$ ($100\ \mu\text{mol L}^{-1}$) in the presence of SeO_3^{2-} ($100\ \mu\text{mol L}^{-1}$). The reduction of $\cdot\text{cPTIO}$ was evaluated as the decrease of the absorbance at $560\ \text{nm}$ after $2.25\ \text{min}$ of the reaction ($\text{pH}\ 7.4$, 37°C). All values represent the means \pm S.E.M., $n = 2\text{--}4$.

increased further in the presence of SeO_3^{2-} (more than three times at a $50/25$ in $\mu\text{mol L}^{-1}$ $\text{H}_2\text{S}/\text{SeO}_3^{2-}$ ratio). This indicates that $\text{H}_2\text{S}/\text{SeO}_3^{2-}$ products scavenge $\text{O}_2^{\cdot-}$ and/or its derivatives. The effects of $\text{H}_2\text{S}/\text{SeO}_3^{2-}$ were less pronounced when KO_2/DMSO was added $5\ \text{min}$ after addition of $\text{H}_2\text{S}/\text{SeO}_3^{2-}$, suggesting that the reducing intermediate had already decomposed at this stage (Figure 5, S4). Similar results were obtained when H_2S was incubated with SeCl_4 (Figure S5). This indicates that the production of highly active species, products of the $\text{H}_2\text{S}/\text{SeO}_3^{2-}$ interaction, was time-dependent: they appeared within a few seconds after addition of SeO_3^{2-} to the H_2S solution and their effects diminished after few minutes of interaction.

From our previous studies of $\text{O}_2^{\cdot-}$ reaction with BMPO [5], we assumed that the EPR spectra of the BMPO adducts were superposed on the BMPO-OOH/OH radicals with minor contribution from the BMPO-C radical. Therefore, we simulated the spectra using hyperfine coupling constants for BMPO-OOH, BMPO-OH, and BMPO-C (derived from DMSO) radicals. The means of hyperfine coupling constants used were as follows: BMPO-OOH1 (black) $a_N = 13.30 \pm 0.03\ \text{G}$, $a_H = 11.7 \pm 0.1\ \text{G}$; BMPO-OOH2 (red) $a_N = 13.24 \pm 0.03\ \text{G}$, $a_H = 9.4 \pm 0.1\ \text{G}$; BMPO-OH1 (green) $a_N = 13.7 \pm 0.3\ \text{G}$, $a_H = 12.3 \pm 0.4\ \text{G}$; BMPO-OH2 (yellow) $a_N = 13.6 \pm 0.2\ \text{G}$, $a_H = 15.3 \pm 0.1\ \text{G}$; and BMPO-C (blue) $a_N = 15.2 \pm 0.1\ \text{G}$, $a_H = 21.5 \pm 0.1\ \text{G}$. The constants are similar to those reported by Zhao et al. [49]. The simulation revealed that $\text{O}_2^{\cdot-}$ was trapped in the control and in the presence of SeO_3^{2-} (Figures 5(a) and 5(b)), since the EPR spectra of BMPO-OOH were only observed. However, BMPO-OH component was present in the samples containing H_2S alone or with SeO_3^{2-} (Figures 5(c)–5(h)). The results may indicate that H_2S alone or with SeO_3^{2-} decomposed BMPO-OOH to BMPO-OH and/or OH was formed as a result of compound presence. Since the first spectrum was recorded $110 \pm 15\ \text{s}$ after sample preparation, we cannot exclude a possibility of trapping of other radicals with lifetimes shorter than $110\ \text{s}$.

3.3. $\text{H}_2\text{S}/\text{SeO}_3^{2-}$ Cleaves pDNA. It was of interest to know if the products of the $\text{H}_2\text{S}/\text{SeO}_3^{2-}$ interaction have biological effects *in vitro*. Therefore, we investigated the direct effects of H_2S and SeO_3^{2-} on the cleavage of pDNA *in vitro* using the Fenton reaction as a positive benchmark control (Figure 6) [5].

Interestingly, neither H_2S ($1\ \text{mmol L}^{-1}$) nor SeO_3^{2-} ($0\text{--}1\ \text{mmol L}^{-1}$) alone significantly cleaved pDNA. In contrast, SeO_3^{2-} in a concentration-dependent manner caused damage to DNA in the presence of $1\ \text{mmol L}^{-1}$ H_2S (Figures 6(a1) and 6(a2)). The observed cleavage of DNA caused by SeO_3^{2-} and H_2S showed a bell-shaped concentration ratio dependence similar to the one observed in the reduction of the $\cdot\text{cPTIO}$ radical. We can suggest that the intermediate responsibility of the action can be a selenopolysulfide with a $\text{H}_2\text{S}:\text{SeO}_3^{2-}$ ratio of $4:1$. In the presence of H_2O_2 , damage to pDNA by H_2S occurs also without SeO_3^{2-} , since H_2O_2 now takes on the role of SeO_3^{2-} as an oxidant, with the simultaneous formation of the $\cdot\text{OH}$ radicals (Figures 6(b1) and 6(b2)). Further evidence for the involvement of radicals may come from the fact that dimethylsulfoxide (DMSO), a known $\cdot\text{OH}$ scavenger [50, 51] frequently employed as solvent in biology, is able to interfere with the damage to DNA (Figures 6(c1) and 6(c2)).

3.4. $\text{H}_2\text{S}/\text{SeO}_3^{2-}$ Modulates Tension of Isolated Thoracic Aorta. As some of our *in vitro* assays indicated an antioxidant activity of the $\text{H}_2\text{S}/\text{SeO}_3^{2-}$ mixture, and H_2S is known to promote relaxation of blood vessels [52], the impact of the $\text{H}_2\text{S}/\text{SeO}_3^{2-}$ mixture on the isolated thoracic aorta was examined. The thoracic aorta was precontracted by noradrenaline (NA) ($1\ \mu\text{mol L}^{-1}$). After a stable plateau of the contraction was reached (Figure 7(a)), SeO_3^{2-} ($100\ \mu\text{mol L}^{-1}$) showed only negligible activity, while Na_2S ($200\ \mu\text{mol L}^{-1}$) significantly relaxed the aortic rings, in agreement with our previous studies [38]. A simultaneous addition of SeO_3^{2-} ($100\ \mu\text{mol L}^{-1}$) and H_2S ($200\ \mu\text{mol L}^{-1}$) resulted once more in a biphasic activity profile, where a minor

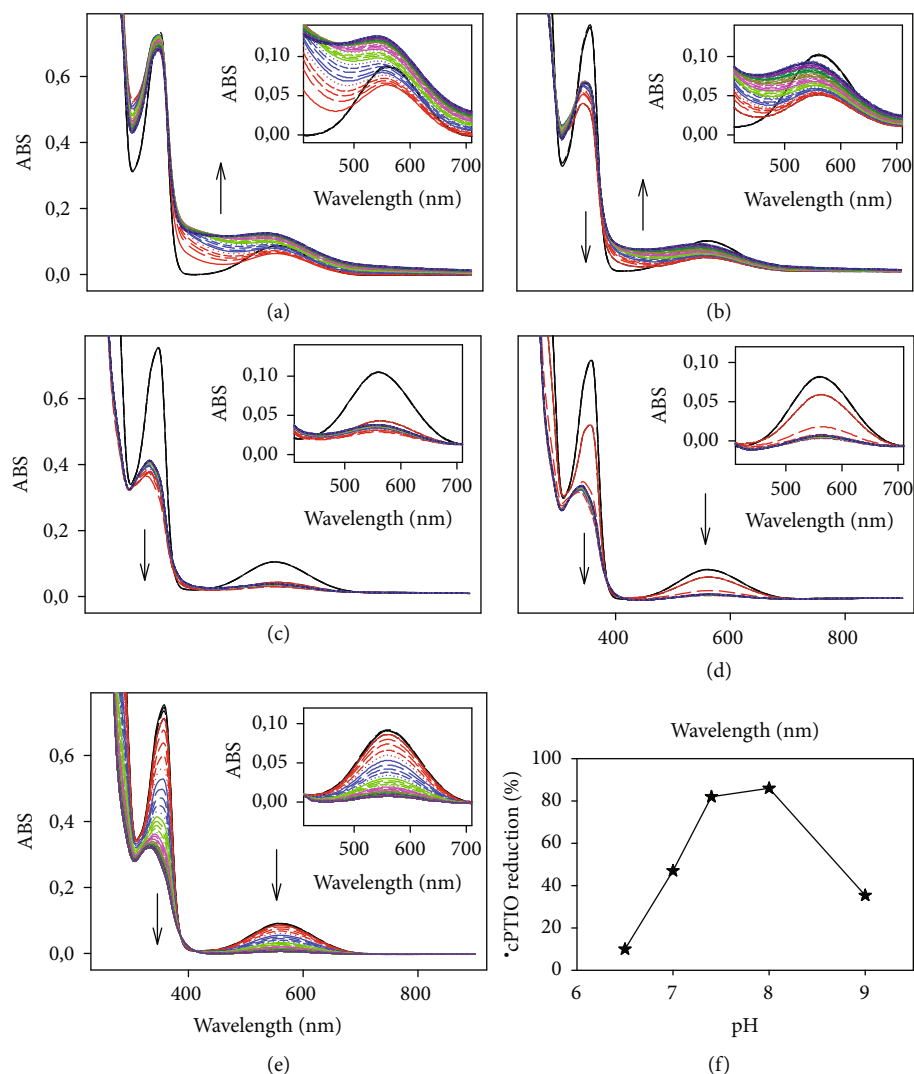


FIGURE 3: Effect of pH on the reduction of \cdot cPTIO in the presence of SeO_3^{2-} induced by H_2S . Time resolved UV-VIS spectra of the interaction of H_2S ($100 \mu\text{mol L}^{-1}$ final) with \cdot cPTIO/ SeO_3^{2-} ($100/50$ in $\mu\text{mol L}^{-1}$ final) at pH 6.5 (a), 7.0 (b), 7.4 (c), 8.0 (d), and 9.0 (e). The first spectrum was recorded 15 s after H_2S addition (solid red line) followed each 30 s by: long dash red, medium dash red, short dash red, dotted red, solid blue line, long dash blue, medium dash blue, etc. Samples were measured every 30 s for 20 min. The black line represents the spectrum of \cdot cPTIO/ SeO_3^{2-} before the H_2S addition. (f) Dependence of \cdot cPTIO ($100 \mu\text{mol L}^{-1}$) reduction by $\text{H}_2\text{S}/\text{SeO}_3^{2-}$ ($100/50$ in $\mu\text{mol L}^{-1}$) on pH. Data were taken from the spectra shown in (a), (b), (c), (d), and (e) as a minimum of A_{560} in the range of 0-4 min. The buffers consisted of 100 mmol L^{-1} sodium phosphate, $100 \mu\text{M}$ DTPA, 37°C , and pH values were adjusted to desired pH.

relaxation was noticed first, followed by a pronounced contraction (Figure 7). It is supposed that the contraction effect may result also from the antioxidant properties of the mixture, similarly as it has been reported for ascorbate [53].

3.5. $\text{H}_2\text{S}/\text{SeO}_3^{2-}$ Modulates Rat Systolic and Pulse Blood Pressure. Since the products of the $\text{H}_2\text{S}/\text{SeO}_3^{2-}$ interaction modulated the tension of the thoracic aorta, we subsequently studied whether the products influence blood pressure (BP). Intravenous (i.v.) administration of $5 \mu\text{mol kg}^{-1}$ SeO_3^{2-} had only minor effects on BP (Figure 8(g)). The administration of $10 \mu\text{mol kg}^{-1}$ of Na_2S transiently decreased and increased BP (Figures 8(a) and 8(g)), as observed in our previous study [54]. The stock solution of the $\text{H}_2\text{S}/\text{SeO}_3^{2-}$ mixture

($20/10$ in mmol L^{-1}) prepared in 0.9% NaCl was colorless and had pH ~ 11 . However, when the mixture was prepared in solution with pH 7.4, it had orange color with an absorption maximum at 570 nm (Figure S6), indicating formation of the sulfur-selenium complexes [40]. The i.v. administration of the mixture $\text{H}_2\text{S}/\text{SeO}_3^{2-}$ ($10/5 \mu\text{mol kg}^{-1}$, pH ~ 7.4), in comparison to H_2S alone, inhibited both BP decrease and increase (Figures 8(b) and 8(g)). The effects of the mixture were less pronounced at pH ~ 11 , being the effects at this pH similar to those observed for H_2S alone (Figures 8(c) and 8(g)).

The studied compounds influenced pulse BP, as an important parameter of cardiovascular system reflecting arterial stiffness [55, 56]. The administration of $5 \mu\text{mol kg}^{-1}$

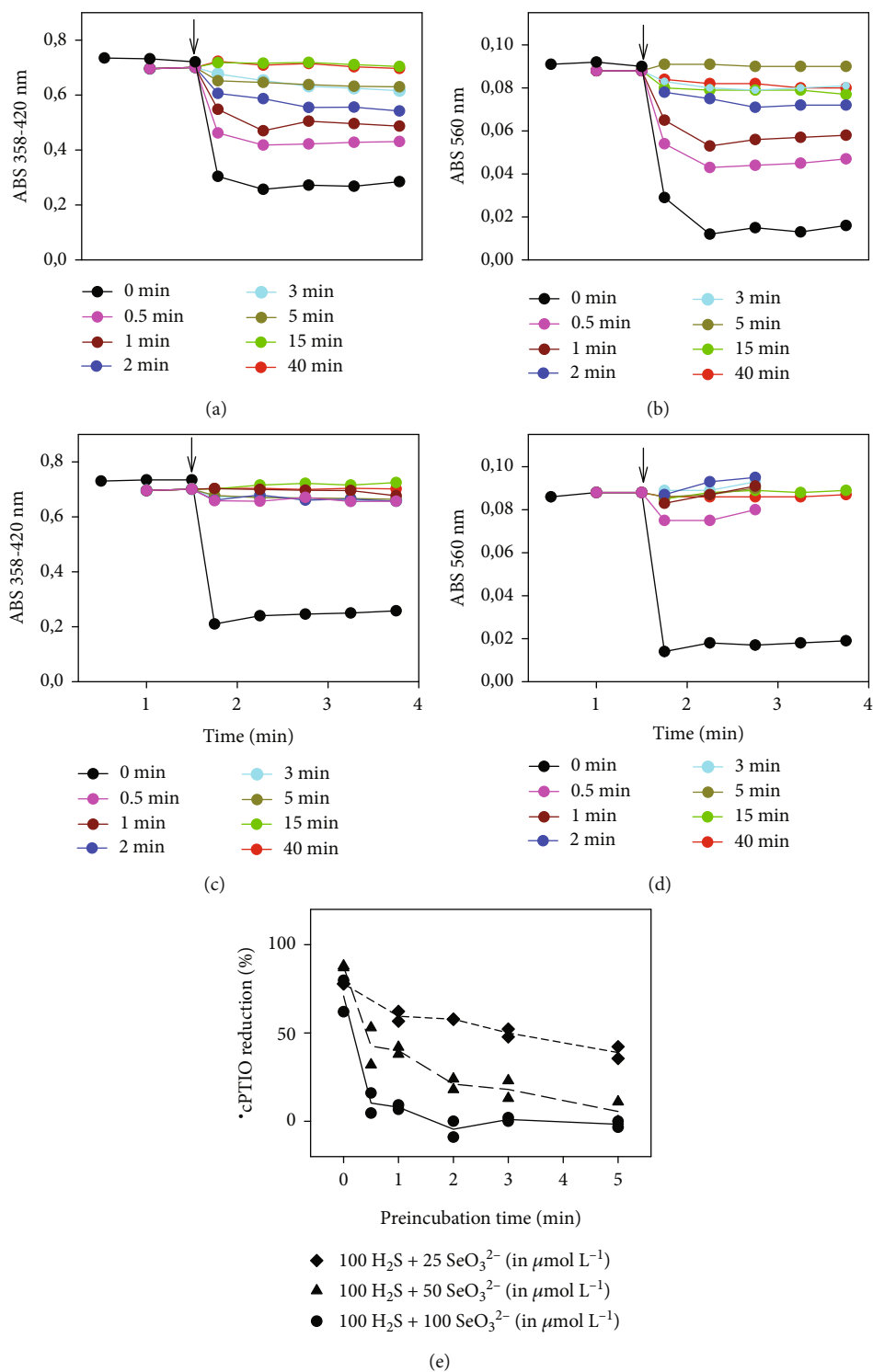


FIGURE 4: Influence of the preincubation time of the $\text{H}_2\text{S}/\text{SeO}_3^{2-}$ mixture on the time-dependent reduction of cPTIO . The reduction of cPTIO ($100 \mu\text{mol L}^{-1}$) once added into the preincubated $\text{H}_2\text{S}/\text{SeO}_3^{2-}$ mixture ($100/50$ in $\mu\text{mol L}^{-1}$, (a, b); $100/100$ in $\mu\text{mol L}^{-1}$ (c, d)) was evaluated as the decrease of absorbance at 358 nm minus 420 nm (a, c) and the decrease of absorbance at 560 nm (b, d), respectively. The preincubation time of the $\text{H}_2\text{S}/\text{SeO}_3^{2-}$ mixture was 0-40 min (see legend). (e) Impact of the preincubation time of the $\text{H}_2\text{S}/\text{SeO}_3^{2-}$ mixture on the reduction of cPTIO . cPTIO ($100 \mu\text{M}$) was added into preincubated $\text{H}_2\text{S}/\text{SeO}_3^{2-}$ (in $\mu\text{mol L}^{-1}$, $100/100$, circles; $100/50$, triangles; $100/25$, diamonds) at $\text{pH } 7.4$, 37°C . Data represent the reduction of cPTIO in 1^{st} minute after addition of cPTIO .

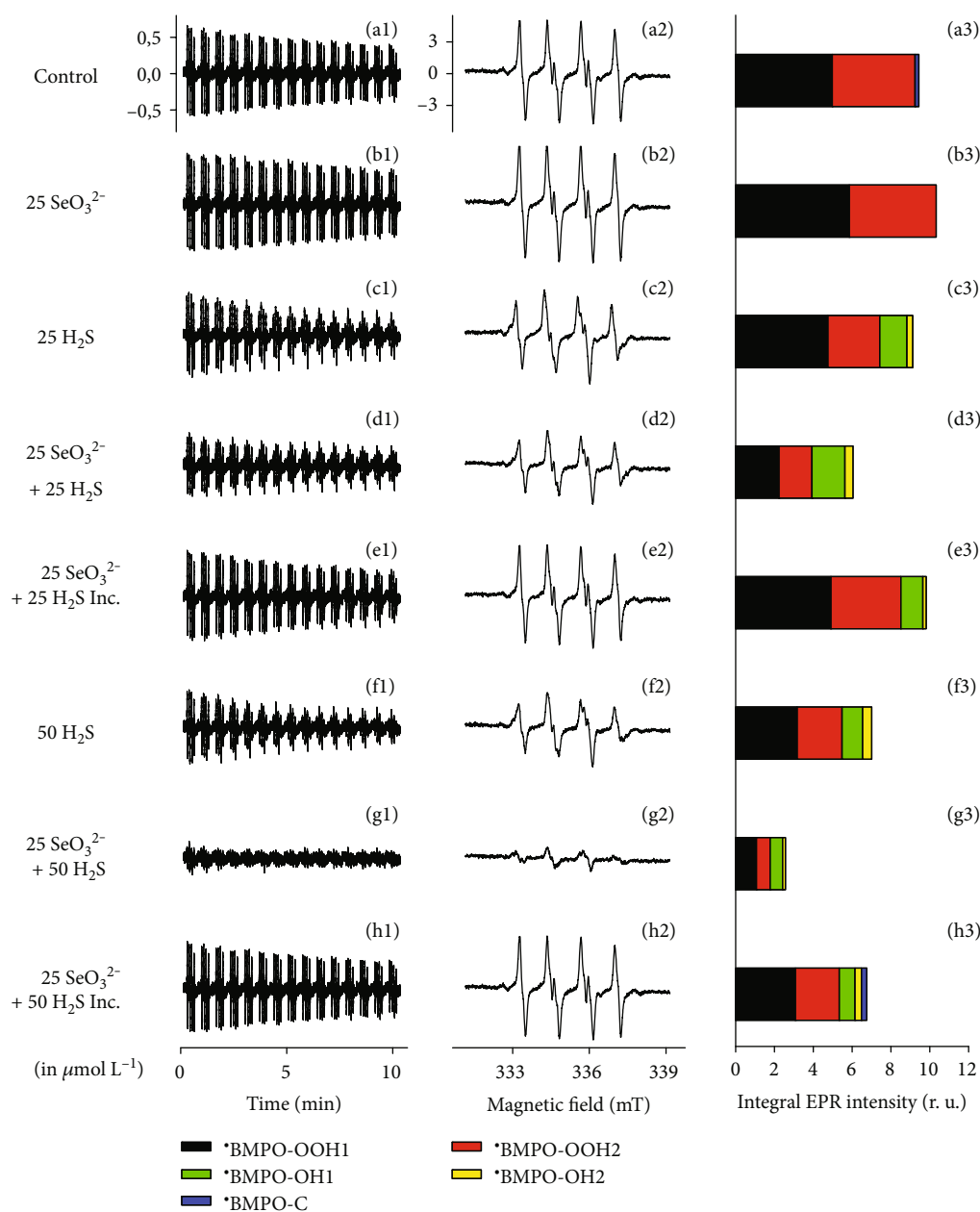


FIGURE 5: EPR spectra of $^{\cdot}BMPO$ in the presence of $O_2^{\cdot -}$ are modulated by H_2S/SeO_3^{2-} . Representative EPR spectra of the $^{\cdot}BMPO$ adducts were monitored in 10% v/v saturated $KO_2/DMSO$ solution in 50 $mmol L^{-1}$ sodium phosphate buffer, 0.1 $mmol L^{-1}$ DTPA, pH 7.4, 37°C in the presence of the various investigated chalcogen species and 20 $mmol L^{-1}$ BMPO. Sets of individual EPR spectra of the $^{\cdot}BMPO$ adducts monitored upon 15 sequential scans, each 42 s (a1-h1), starting acquisition 2 min after sample preparation in: control 10% v/v $KO_2/DMSO$ in the buffer (a1), the $KO_2/DMSO$ in the presence of 25 $\mu mol L^{-1}$ SeO_3^{2-} (b1), 25 $\mu mol L^{-1}$ H_2S (c1), mixture of 25/25 in $\mu mol L^{-1}$ H_2S/SeO_3^{2-} (d1), 25/25 in $\mu mol L^{-1}$ H_2S/SeO_3^{2-} preincubated 5 min before $KO_2/DMSO$ stock solution addition (e1), 50 $\mu mol L^{-1}$ H_2S (f1), mixture of 50/25 in $\mu mol L^{-1}$ H_2S/SeO_3^{2-} (g1), and 50/25 in $\mu mol L^{-1}$ H_2S/SeO_3^{2-} preincubated 5 min before addition of $KO_2/DMSO$ stock solution (h1). The spectra (a2-h2) show details of the accumulated first ten spectra of the (a1-h1) sets. The intensities of the time-dependent EPR spectra (a1-h1) and detailed spectra (a2-h2) are comparable; they were measured under identical EPR settings. EPR modulation amplitude 0.15 mT. (a3-h3) Comparison of the integral intensity of individual components of simulated BMPO+ $O_2^{\cdot -}$ without (control) and with chalcogen species shown in (a1-h1). The first five EPR spectra were accumulated and used for simulation. The data represent the means of $n = 2$; standard error was $\leq 10\%$ of the mean value. Simulated relative intensities of the two conformers of the radicals: BMPO-OOH1 (black), BMPO-OOH2 (red), BMPO-OH1 (green), BMPO-OH2 (yellow), and BMPO-C (blue).

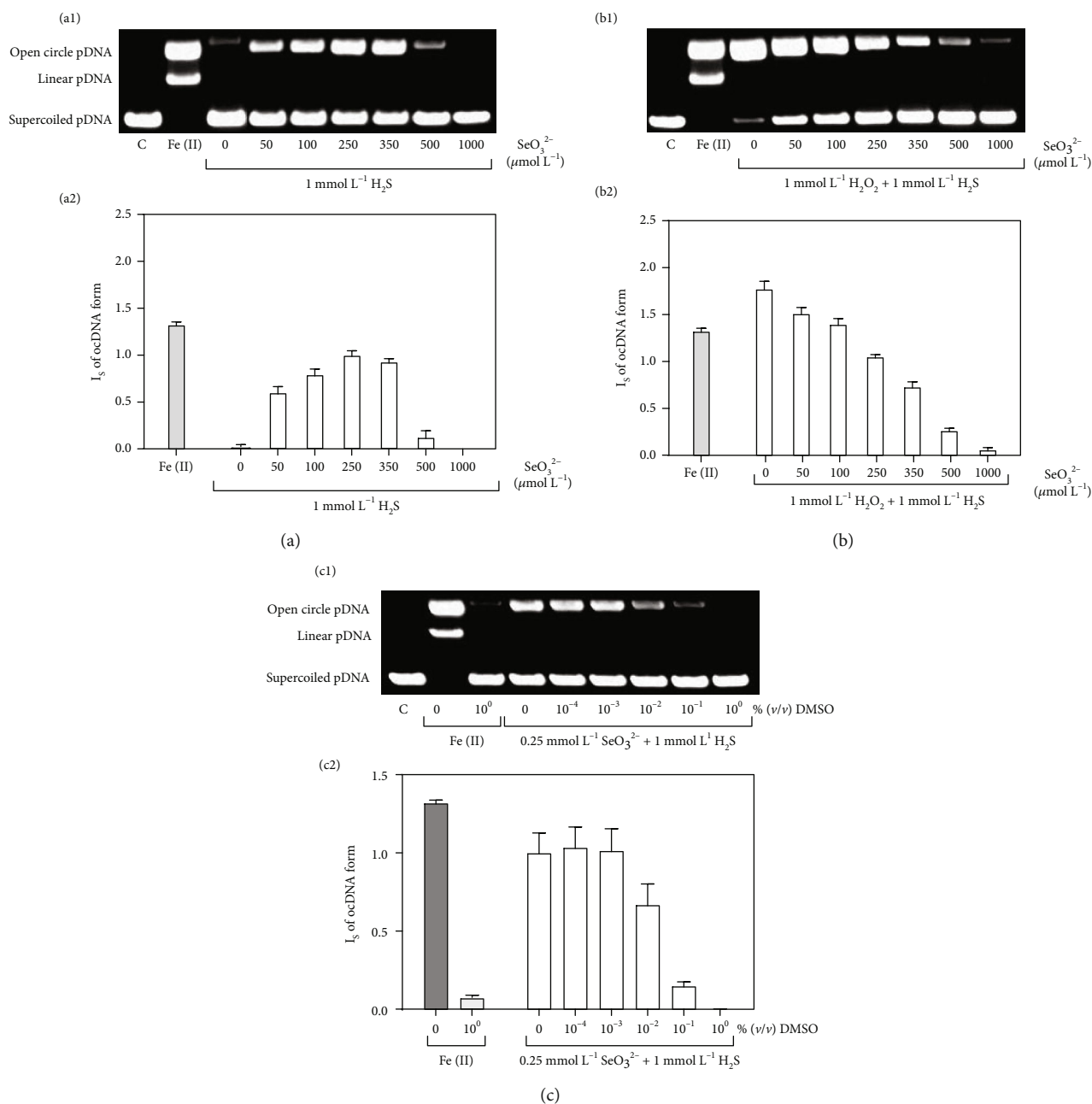


FIGURE 6: The influence of $\text{H}_2\text{S}/\text{SeO}_3^{2-}$ on pDNA cleavage in the absence and presence of H_2O_2 and DMSO. Representative gels (a1, b1) and column graphs (a2, b2) indicating the effects of increasing concentrations of SeO_3^{2-} (0–1 mmol L^{-1}) on pDNA cleavage in the presence of $1 \text{ mmol L}^{-1} \text{H}_2\text{S}$, without (a1, a2) and with $1 \text{ mmol L}^{-1} \text{H}_2\text{O}_2$ (b1, b2). The band at the bottom corresponds to the circular supercoiled form of pDNA, and the less intense band appearing above, in the case of $\text{Fe}^{2+}\text{-H}_2\text{O}_2$, represents the linear form of pDNA. The top band corresponds to the nicked circular form of pDNA. The effects of $150 \mu\text{mol L}^{-1} \text{FeCl}_2 + 1 \text{ mmol L}^{-1} \text{H}_2\text{O}_2$ (full column) are shown for comparison. Values are the means \pm S.E.M., $n = 3$. Representative gels (c1) and column graph (c2) showing the effects of increasing concentrations of DMSO on $\text{H}_2\text{S}/\text{SeO}_3^{2-}$ (0.25/1 in mmol L^{-1})-induced pDNA cleavage. DMSO concentrations: $1 \times 10^{-4}\%$ (v/v) DMSO = $14.1 \mu\text{mol L}^{-1}$ DMSO; $1 \times 10^{-3}\%$ = $141 \mu\text{mol L}^{-1}$; $1 \times 10^{-2}\%$ = 1.41 mmol L^{-1} ; $1 \times 10^{-1}\%$ = 14.1 mmol L^{-1} ; $1 \times 10^0\%$ = 141 mmol L^{-1} . Values represent means \pm S.E.M., $n = 4$.

SeO_3^{2-} intravenously had minor effects on pulse BP (Figure 8(h)). The administration of $10 \mu\text{mol kg}^{-1}$ of Na_2S transiently increased and later decreased pulse BP (Figures 8(d) and 8(h)) [54]. The i.v. administration of the mixture $\text{H}_2\text{S}/\text{SeO}_3^{2-}$ (10/5 in $\mu\text{mol kg}^{-1}$, pH ~ 7.4), with

comparison to H_2S alone, eliminated pulse BP increase, but did not affect pulse BP decrease (Figures 8(e) and 8(h)). The effects of the mixture were less pronounced at pH ~ 11 and were similar to those observed for H_2S alone (Figures 8(f) and 8(h)). The inefficiency of the

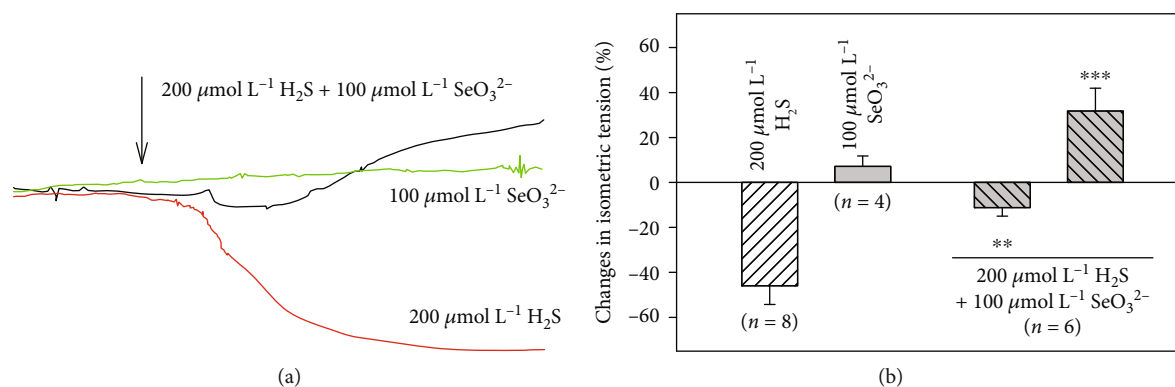


FIGURE 7: Time-dependent tonus of isolated thoracic aorta. The original records of changes in NA ($1 \mu\text{mol L}^{-1}$)-increased arterial tone of isolated rat thoracic aorta after addition of SeO_3^{2-} ($100 \mu\text{mol L}^{-1}$), H_2S ($200 \mu\text{mol L}^{-1}$), and $\text{H}_2\text{S}/\text{SeO}_3^{2-}$ ($200/100$ in $\mu\text{mol L}^{-1}$) mixture. The arrow indicates the compound application (a). The effects of SeO_3^{2-} , H_2S , and $\text{H}_2\text{S}/\text{SeO}_3^{2-}$ on NA ($1 \mu\text{mol L}^{-1}$)-precontracted rings of rat thoracic aorta. The rings were exposed to bolus dose of H_2S ($200 \mu\text{mol L}^{-1}$, relaxation), SeO_3^{2-} ($100 \mu\text{mol L}^{-1}$, nonsignificant contraction), and that of the mixture $\text{H}_2\text{S}/\text{SeO}_3^{2-}$ ($100 \mu\text{mol L}^{-1}$ of SeO_3^{2-} immediately followed by $200 \mu\text{mol L}^{-1}$ H_2S). The $\text{SeO}_3^{2-}/\text{H}_2\text{S}$ mixture had a biphasic activity; firstly, it significantly relaxed the aorta, which was followed by significant contraction (b). Asterisks mark the statistical significance of $\text{H}_2\text{S}/\text{SeO}_3^{2-}$ mixture vs. H_2S (** $P < 0.01$, *** $P < 0.001$).

$\text{H}_2\text{S}/\text{SeO}_3^{2-}$ products at pH ~ 11 may be connected with the minor effect of the mixture on the $\cdot\text{cPTIO}$ radical reduction at high pH (Figures 3(e) and 3(f)). This may imply that the reduction properties of the mixture could be responsible for their effects on systolic and pulse BP. The results confirm that the products of the $\text{H}_2\text{S}/\text{SeO}_3^{2-}$ interaction depend on pH and influence differently the cardiovascular system. In conclusion, the reactivity and biological activity of the $\text{H}_2\text{S}/\text{SeO}_3^{2-}$ interaction products prepared at pH 7.4 differ from those of Na_2S alone.

4. Discussion and Conclusions

Overall, our studies demonstrate that the two suspected and commonly used “antioxidants,” H_2S and SeO_3^{2-} , are not necessarily typical reducing agents, such as ascorbic acid or tocopherol, when employed on their own. Interestingly, these two chalcogen agents, when added together, rapidly activate each other and form a cascade of considerably more reactive, often reducing species, supposing the involvement of inorganic HSSeSH and polysulfides S_x^{2-} , which may account for some of the observed biological actions. The nature of some of these intermediate reactive sulfur and/or selenium species was suggested in a recently published review [40].

The fast and efficient reduction of the $\cdot\text{cPTIO}$ radical by $\text{H}_2\text{S}/\text{SeO}_3^{2-}$ products (Figures 1 and 4) supports the notion that the initial intermediate(s) formed by the reaction of H_2S with SeO_3^{2-} are responsible for this kind of action. The bell shape and the maximum radical scavenging activity of $\text{H}_2\text{S}:\text{SeO}_3^{2-}$ at a ratio of $\sim 4:1$ (Figure 2) may indicate the suggested formation of $(\text{HSS})_2\text{Se}$ [40]. The kinetics and efficiency of the $\text{H}_2\text{S}/\text{SeO}_3^{2-}$ products to reduce $\cdot\text{cPTIO}$ (Figure 3) point out to complex pH-dependent chemical and radical reactions of the species.

Reactions of H_2S or polysulfides with SeO_3^{2-} and/or SeCl_4 were reported [40, 57–59]. They point towards a rapid

conversion of SeO_3^{2-} and SeCl_4 to an intermediate, probably HSSeSH, and a subsequent, slower reductive elimination of this intermediate to elemental (mixed) chalcogen particles and disulfides [40]. However, to our knowledge, there is no information about the formation and detection of HSSeSH in cells or its cytoprotective or other biological effect. The first synthesis of H-S-Se-S-H (1,3-dithiatriselane) was reported by Hahn and Klünsch in 1994, but the stability and reactivity in aqueous solution were not investigated. Solid HSSeSH has a melting point at -40°C . It was one component of a mixture of $\text{H}_2\text{S}_2\text{Se}_n$, prepared by the interaction of 2 H_2S with Se_2Cl_2 [60].

The EPR data (Figure 5) once more confirm that SeO_3^{2-} on its own is not an antioxidant; it becomes activated by reduction, for instance, by H_2S , which concurrently is activated by oxidation. The mutual redox activation is fast, and, as in the case of the $\cdot\text{cPTIO}$ radical scavenging, the pristine mixture of H_2S and SeO_3^{2-} is most active, with a decrease of activity over the time, pointing once more at simple H_2S_x or $\text{H}_2\text{S}_x\text{Se}$, and notably HSSeSH, but not an S_xSe_y , as being responsible for this kind of activity.

We found that the products of this described $\text{H}_2\text{S}/\text{SeO}_3^{2-}$ interaction have several noteworthy biological effects, involving ROS scavenging, modulation of the redox state, reaction with DNA, tensing isolated aorta, and influencing BP and pulse BP (Figures 6–8). These effects obviously need to be investigated further and in considerably more detail and were not present or were less pronounced when H_2S or selenite acted alone. The properties of the products of the $\text{H}_2\text{S}/\text{SeO}_3^{2-}$ interactions significantly depended on the $\text{H}_2\text{S}/\text{SeO}_3^{2-}$ molar ratio, pH, and preincubation time. The combination of these variables makes the work with $\text{H}_2\text{S}/\text{SeO}_3^{2-}$ very complicated, and these facts should be taken into account at the time of designing *in vitro* and *in vivo* experiments. These properties of the products may explain the previously published beneficial and contrasting toxic Se

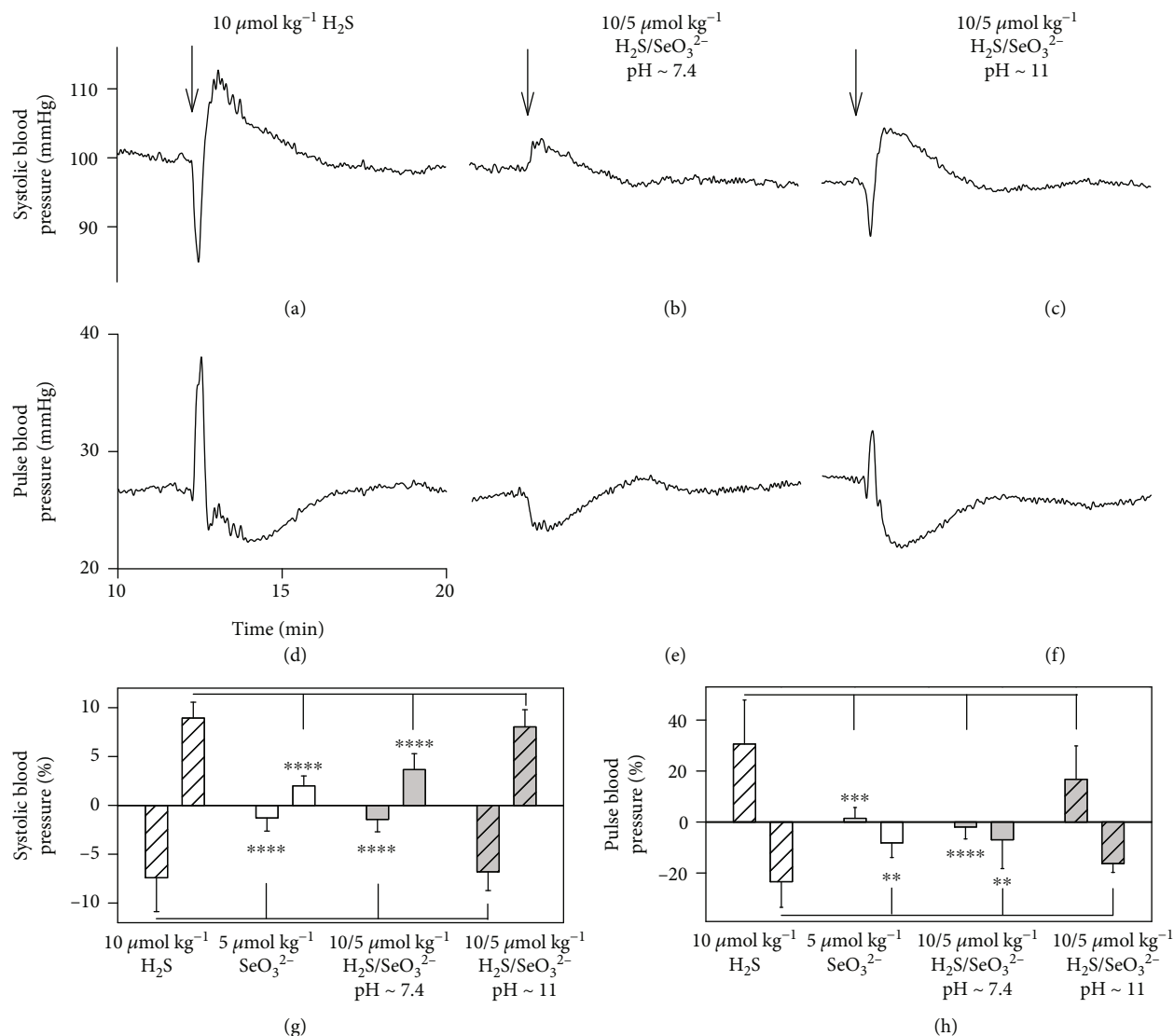


FIGURE 8: The time-dependent effects of SeO₃²⁻, H₂S, and H₂S/SeO₃²⁻ on rat BP and pulse BP. Representative traces of the time-dependent effect of i.v. bolus administration of H₂S (10 μmol kg⁻¹; (a, d)) and its mixture with 5 μmol kg⁻¹ SeO₃²⁻ prepared at pH ~ 7.4 (b, e) and pH ~ 11 (c, f) solution on BP (a, b, c) and pulse BP (d, e, f). Transient changes of rat BP (g) and pulse BP (h) after i.v. bolus administration of SeO₃²⁻ (5 μmol kg⁻¹, empty column), H₂S (10 μmol kg⁻¹, empty coarse column) and their mixture (SeO₃²⁻/H₂S, 5/10 in μmol kg⁻¹) prepared at pH ~ 7.4 (grey column) and pH ~ 11 (grey coarse column). Data are presented as means ± SD; n = 5-10. To test a statistical significance between group differences, we used one-way ANOVA followed by Dunnett's test for multiple comparisons. Hence, we also observed the biphasic effect of Na₂S in our previous study [54]; we compared a set of "first part" and "second part" effects of SeO₃²⁻, H₂S/SeO₃²⁻ at pH ~ 7.4, and H₂S/SeO₃²⁻ at pH ~ 11.0 to the corresponding effect of Na₂S on systolic or pulse blood pressure. Only the mixture of H₂S/SeO₃²⁻ prepared at pH ~ 11.0 was able to generate similar decrease and subsequent increase or *vice versa* in systolic blood pressure or pulse blood pressure as the H₂S, respectively. Asterisks mark the statistical significance as follows: **P < 0.01, ***P < 0.001, and ****P < 0.0001.

effects, for example, in conditions of oxidative stress and cancer [12-14, 18, 20, 22, 23, 30].

H₂S is endogenously produced *in vivo* in most, if not in all, cells, and H₂S donors are commonly used in biological experiments, and they are considered to be applied in medicine. Our results suggest that in biological experiments with selenite, in its nutrition supplement and clinical use, effects of the H₂S/SeO₃²⁻ interaction should be considered. While SeO₃²⁻ is used widely as a nutritional supplement already,

one may, in the future, wish to spice it up with some reduced sulfur. Natural spices such as garlic and onions contain suitable sulfide releasing agents, such as diallyltrisulfide (DATS) and diallyltetrasulfide (DATTS), which both occur naturally in garlic, or dipropyltrisulfide and dipropyltetrasulfide, both present in onions [61]. Our results imply that application research of suitable H₂S/SeO₃²⁻ supplements may lead to the beneficial effects in pathological conditions arising, e.g., from ROS overproduction.

Abbreviations

ABS:	Absorbance
BMPO:	5- <i>tert</i> -butoxycarbonyl-5-methyl-1-pyrroline- <i>N</i> -oxide
BP:	Blood pressure
¹³ CPTIO:	2-(4-Carboxyphenyl)-4,4,5,5-tetramethylimidazo- line-1-oxyl-3-oxide
DTPA:	Diethylenetriaminepentaacetic acid
EPR:	Electron paramagnetic resonance
H ₂ S:	Hydrogen sulfide
H ₂ O ₂ :	Hydrogen peroxide
i.p.:	Intraperitoneal
i.v.:	Intravenous
NA:	Noradrenaline
pDNA:	Plasmid DNA
SeCl ₄ :	Selenium tetrachloride
SeO ₃ ²⁻ :	Selenite
UV/VIS:	Ultraviolet-visible.

Data Availability

All findings and conclusions are based on the presented figures in the main text or in the supplementary information. Original source files (UV-VIS spectra, EPR spectra, DNA gels, rat blood pressure records, and aorta relaxation records) can be sent from the corresponding author, Dr. Karol Ondrias, upon request.

Conflicts of Interest

The authors declare no conflict of interest.

Authors' Contributions

K.O. and M.C. conceived, initiated, and coordinated the study; K.O., M.C. and V.B. designed research; K.O., M.G., A.M., and A.K. performed UV-VIS experiments and analyzed data; V.B., K.O., M.G., and A.M. performed EPR experiments and analyzed data; M.C. and A.M. performed pDNA cleavage experiments and analyzed data; L.T., A.M, K.O., S.C., A.B., and P.B. performed aorta experiments and analyzed data; L.K., A.M., S.C., A.B., and K.O. performed rat *in vivo* experiments. K.O. wrote the paper; K.O., M.C., V.B., A.K., and E.A-D contributed to analyze data and manuscript writing. Marian Grman and Anton Misak contributed equally to this work. Miroslav Chovanec and Karol Ondrias shared senior authorship.

Acknowledgments

This research was funded by the Slovak Research and Development Agency (grant numbers APVV-15-0371 to A.M., M.G., and K.O.; APVV-17-0384 to M.C.; and APVV-15-0565 to A.M, S.C., A.B., and P.B.), the VEGA Grant Agency of the Slovak Republic (grant numbers 2/0079/19 to M.G.; 1/0026/18 to V.B.; 2/0053/19 to M.C.; and 2/0014/17 to K.O.), and University Science Park for Biomedicine (ITMS 26240220087).

Supplementary Materials

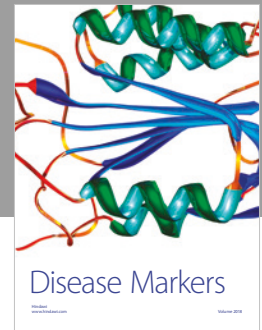
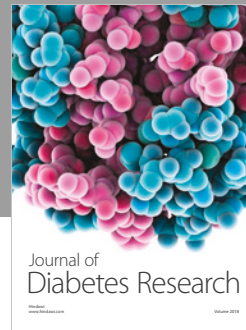
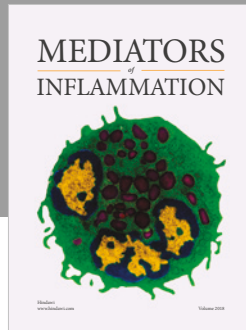
The supplementary information's file (PDF) contains only additional figures with legends to the main manuscript text. (*Supplementary Materials*)

References

- [1] R. Wang, "Physiological implications of hydrogen sulfide: a whiff exploration that blossomed," *Physiological Reviews*, vol. 92, no. 2, pp. 791–896, 2012.
- [2] C. Szabo and A. Papapetropoulos, "International union of basic and clinical pharmacology. CII: pharmacological modulation of H₂S levels: H₂S donors and H₂S biosynthesis inhibitors," *Pharmacological Reviews*, vol. 69, no. 4, pp. 497–564, 2017.
- [3] L. Tomasova, P. Konopelski, and M. Ufnal, "Gut bacteria and hydrogen sulfide: the new old players in circulatory system homeostasis," *Molecules*, vol. 21, no. 11, p. 1558, 2016.
- [4] Y.-H. Liu, M. Lu, L.-F. Hu, P. T.-H. Wong, G. D. Webb, and J.-S. Bian, "Hydrogen sulfide in the mammalian cardiovascular system," *Antioxidants and Redox Signaling*, vol. 17, no. 1, pp. 141–185, 2012.
- [5] A. Misak, M. Grman, Z. Bacova et al., "Polysulfides and products of H₂S/S-nitrosoglutathione in comparison to H₂S, glutathione and antioxidant Trolox are potent scavengers of superoxide anion radical and produce hydroxyl radical by decomposition of H₂O₂," *Nitric Oxide*, vol. 76, pp. 136–151, 2018.
- [6] A. Staško, V. Brezová, M. Zalibera, S. Biskupič, and K. Ondriaš, "Electron transfer: a primary step in the reactions of sodium hydrosulphide, an H₂S/HS⁻ donor," *Free Radical Research*, vol. 43, no. 6, pp. 581–593, 2009.
- [7] M. Whiteman, J. S. Armstrong, S. H. Chu et al., "The novel neuromodulator hydrogen sulfide: an endogenous peroxynitrite 'scavenger?'," *Journal of Neurochemistry*, vol. 90, no. 3, pp. 765–768, 2004.
- [8] M. Whiteman, N. S. Cheung, Y.-Z. Zhu et al., "Hydrogen sulphide: a novel inhibitor of hypochlorous acid-mediated oxidative damage in the brain?," *Biochemical and Biophysical Research Communications*, vol. 326, no. 4, pp. 794–798, 2005.
- [9] M. A. Eghbal, P. S. Pennefather, and P. J. O'Brien, "H₂S cytotoxicity mechanism involves reactive oxygen species formation and mitochondrial depolarisation," *Toxicology*, vol. 203, no. 1–3, pp. 69–76, 2004.
- [10] D. H. Truong, M. A. Eghbal, W. Hindmarsh, S. H. Roth, and P. J. O'Brien, "Molecular mechanisms of hydrogen sulfide toxicity," *Drug Metabolism Reviews*, vol. 38, no. 4, pp. 733–744, 2006.
- [11] J. Jiang, A. Chan, S. Ali et al., "Hydrogen sulfide—mechanisms of toxicity and development of an antidote," *Scientific Reports*, vol. 6, no. 1, 2016.
- [12] S. Miller, S. W. Walker, J. R. Arthur et al., "Selenite protects human endothelial cells from oxidative damage and induces thioredoxin reductase," *Clinical Science*, vol. 100, no. 5, pp. 543–550, 2001.
- [13] R. S. Lymbury, M. J. Marino, and A. V. Perkins, "Effect of dietary selenium on the progression of heart failure in the ageing spontaneously hypertensive rat," *Molecular Nutrition & Food Research*, vol. 54, no. 10, pp. 1436–1444, 2010.

- [14] S. J. Fairweather-Tait, Y. Bao, M. R. Broadley et al., "Selenium in human health and disease," *Antioxidants and Redox Signaling*, vol. 14, no. 7, pp. 1337–1383, 2011.
- [15] J. Bleys, A. Navas-Acien, and E. Guallar, "Serum selenium and diabetes in U.S. adults," *Diabetes Care*, vol. 30, no. 4, pp. 829–834, 2007.
- [16] G. Deyab, I. Hokstad, J. Aaseth et al., "Effect of anti-rheumatic treatment on selenium levels in inflammatory arthritis," *Journal of Trace Elements in Medicine and Biology*, vol. 49, pp. 91–97, 2018.
- [17] R. A. Heller, J. Seelig, T. Bock et al., "Relation of selenium status to neuro-regeneration after traumatic spinal cord injury," *Journal of Trace Elements in Medicine and Biology*, vol. 51, pp. 141–149, 2019.
- [18] Clark, Dalkin, Krongrad et al., "Decreased incidence of prostate cancer with selenium supplementation: results of a double-blind cancer prevention trial," *British Journal of Urology*, vol. 81, no. 5, pp. 730–734, 1998.
- [19] S. M. Lippman, E. A. Klein, P. J. Goodman et al., "Effect of selenium and vitamin E on risk of prostate cancer and other cancers," *JAMA*, vol. 301, no. 1, pp. 39–51, 2009.
- [20] M. Vinceti, T. Filippini, C. Del Giovane et al., "Selenium for preventing cancer," *Cochrane Database of Systematic Reviews*, no. 3, Article CD005195, 2014.
- [21] N. Karunasinghe, S. Zhu, and L. R. Ferguson, "Benefits of selenium supplementation on leukocyte DNA integrity interact with dietary micronutrients: a short communication," *Nutrients*, vol. 8, no. 5, p. 249, 2016.
- [22] J. Lü, J. Zhang, C. Jiang, Y. Deng, N. Özten, and M. C. Bosland, "Cancer chemoprevention research with selenium in the post-SELECT era: promises and challenges," *Nutrition and Cancer*, vol. 68, no. 1, pp. 1–17, 2016.
- [23] J. K. Wrobel, R. Power, and M. Toborek, "Biological activity of selenium: revisited," *IUBMB Life*, vol. 68, no. 2, pp. 97–105, 2016.
- [24] R. R. Ramoutar and J. L. Brumaghim, "Effects of inorganic selenium compounds on oxidative DNA damage," *Journal of Inorganic Biochemistry*, vol. 101, no. 7, pp. 1028–1035, 2007.
- [25] C. Jiang, H. Hu, B. Malewicz, Z. Wang, and J. Lü, "Selenite-induced p53 ser-15 phosphorylation and caspase-mediated apoptosis in LNCaP human prostate cancer cells," *Molecular Cancer Therapeutics*, vol. 3, no. 7, pp. 877–884, 2004.
- [26] J. Lu, M. Kaeck, C. Jiang, A. C. Wilson, and H. J. Thompson, "Selenite induction of DNA strand breaks and apoptosis in mouse leukemic L1210 cells," *Biochemical Pharmacology*, vol. 47, no. 9, pp. 1531–1535, 1994.
- [27] J. J. An, K. J. Shi, W. Wei et al., "The ROS/JNK/ATF2 pathway mediates selenite-induced leukemia NB4 cell cycle arrest and apoptosis *in vitro* and *in vivo*," *Cell Death and Disease*, vol. 4, no. 12, 2013.
- [28] G. Nilsson, X. Sun, C. Nyström et al., "Selenite induces apoptosis in sarcomatoid malignant mesothelioma cells through oxidative stress," *Free Radical Biology and Medicine*, vol. 41, no. 6, pp. 874–885, 2006.
- [29] S. Biswas, G. Talukder, and A. Sharma, "Chromosome damage induced by selenium salts in human peripheral lymphocytes," *Toxicology In Vitro*, vol. 14, no. 5, pp. 405–408, 2000.
- [30] J. Brozmanová, D. Mániková, V. Vlčková, and M. Chovanec, "Selenium: a double-edged sword for defense and offence in cancer," *Archives of Toxicology*, vol. 84, no. 12, pp. 919–938, 2010.
- [31] E. Jablonska and M. Vinceti, "Selenium and human health: witnessing a Copernican revolution?," *Journal of Environmental Science and Health, Part C*, vol. 33, no. 3, pp. 328–368, 2015.
- [32] S. Koike, Y. Ogasawara, N. Shibuya, H. Kimura, and K. Ishii, "Polysulfide exerts a protective effect against cytotoxicity caused by *t*-butylhydroperoxide through Nrf2 signaling in neuroblastoma cells," *FEBS Letters*, vol. 587, no. 21, pp. 3548–3555, 2013.
- [33] W. H. Sun, F. Liu, Y. Chen, and Y. C. Zhu, "Hydrogen sulfide decreases the levels of ROS by inhibiting mitochondrial complex IV and increasing SOD activities in cardiomyocytes under ischemia/reperfusion," *Biochemical and Biophysical Research Communications*, vol. 421, no. 2, pp. 164–169, 2012.
- [34] P. Nagy, Z. Pálinkás, A. Nagy, B. Budai, I. Tóth, and A. Vasas, "Chemical aspects of hydrogen sulfide measurements in physiological samples," *Biochimica et Biophysica Acta (BBA) - General Subjects*, vol. 1840, no. 2, pp. 876–891, 2014.
- [35] U. Samuni, Y. Samuni, and S. Goldstein, "On the distinction between nitroxyl and nitric oxide using nitronyl nitroxides," *Journal of the American Chemical Society*, vol. 132, no. 24, pp. 8428–8432, 2010.
- [36] A. Misak, L. Kurakova, E. Goffa et al., "Sulfide (Na₂S) and polysulfide (Na₂S₂) interacting with doxycycline produce/scavenge superoxide and hydroxyl radicals and induce/inhibit DNA cleavage," *Molecules*, vol. 24, no. 6, p. 1148, 2019.
- [37] D. Grundy, "Principles and standards for reporting animal experiments in *The Journal of Physiology and Experimental Physiology*," *Journal of Physiology*, vol. 593, no. 12, pp. 2547–2549, 2015.
- [38] S. Cacanyiova, A. Berenyiova, F. Kristek, M. Drobna, K. Ondrias, and M. Grman, "The adaptive role of nitric oxide and hydrogen sulphide in vasoactive responses of thoracic aorta is triggered already in young spontaneously hypertensive rats," *Journal of Physiology and Pharmacology*, vol. 67, no. 4, pp. 501–512, 2016.
- [39] L. Tomasova, M. Pavlovicova, L. Malekova et al., "Effects of AP39, a novel triphenylphosphonium derivatised anethole dithiolethione hydrogen sulfide donor, on rat haemodynamic parameters and chloride and calcium Ca_v3 and RyR2 channels," *Nitric Oxide*, vol. 46, pp. 131–144, 2015.
- [40] A. Kharma, M. Grman, A. Misak et al., "Inorganic polysulfides and related reactive sulfur-selenium species from the perspective of chemistry," *Molecules*, vol. 24, no. 7, 2019.
- [41] K. A. Cupp-Sutton and M. T. Ashby, "Biological chemistry of hydrogen selenide," *Antioxidants*, vol. 5, no. 4, 2016.
- [42] X. Pan, X. Song, C. Wang et al., "H₂Se induces reductive stress in HepG2 cells and activates cell autophagy by regulating the redox of HMGB1 protein under hypoxia," *Theranostics*, vol. 9, no. 6, pp. 1794–1808, 2019.
- [43] C. L. Bianco, T. A. Chavez, V. Sosa et al., "The chemical biology of the persulfide (RSSH)/perthiyl (RSS[•]) redox couple and possible role in biological redox signaling," *Free Radical Biology and Medicine*, vol. 101, pp. 20–31, 2016.
- [44] D. J. O'Brien and F. B. Birkner, "Kinetics of oxygenation of reduced sulfur species in aqueous solution," *Environmental Science & Technology*, vol. 11, no. 12, pp. 1114–1120, 1977.
- [45] K. L. Nuttall and F. S. Allen, "Kinetics of the reaction between hydrogen selenide ion and oxygen," *Inorganica Chimica Acta*, vol. 91, no. 4, pp. 243–246, 1984.

- [46] G. W. Luther, A. J. Findlay, D. J. MacDonald et al., "Thermodynamics and kinetics of sulfide oxidation by oxygen: a look at inorganically controlled reactions and biologically mediated processes in the environment," *Frontiers in Microbiology*, vol. 2, 2011.
- [47] J. M. Fukuto, S. J. Carrington, D. J. Tantillo et al., "Small molecule signaling agents: the integrated chemistry and biochemistry of nitrogen oxides, oxides of carbon, dioxygen, hydrogen sulfide, and their derived species," *Chemical Research in Toxicology*, vol. 25, no. 4, pp. 769–793, 2012.
- [48] S. S. Saund, V. Sosa, S. Henriquez et al., "The chemical biology of hydropersulfides (RSSH): chemical stability, reactivity and redox roles," *Archives of Biochemistry and Biophysics*, vol. 588, pp. 15–24, 2015.
- [49] H. Zhao, J. Joseph, H. Zhang, H. Karoui, and B. Kalyanaraman, "Synthesis and biochemical applications of a solid cyclic nitron spin trap: a relatively superior trap for detecting superoxide anions and glutathyl radicals," *Free Radical Biology and Medicine*, vol. 31, no. 5, pp. 599–606, 2001.
- [50] J. E. Repine, O. W. Pfenninger, D. W. Talmage, E. M. Berger, and D. E. Pettijohn, "Dimethyl sulfoxide prevents DNA nicking mediated by ionizing radiation or iron/hydrogen peroxide-generated hydroxyl radical," *Proceedings of the National Academy of Sciences*, vol. 78, no. 2, pp. 1001–1003, 1981.
- [51] M. Noda, Y. Ma, Y. Yoshikawa et al., "A single-molecule assessment of the protective effect of DMSO against DNA double-strand breaks induced by photo- and γ -ray-irradiation, and freezing," *Scientific Reports*, vol. 7, no. 1, 2017.
- [52] S. Cacanyiova, A. Berenyiova, P. Balis et al., "Nitroso-sulfide coupled signaling triggers specific vasoactive effects in the intrarenal arteries of patients with arterial hypertension," *Journal of Physiology and Pharmacology*, vol. 68, no. 4, pp. 527–538, 2017.
- [53] P. F. Dillon, R. S. Root-Bernstein, and C. M. Lieder, "Antioxidant-independent ascorbate enhancement of catecholamine-induced contractions of vascular smooth muscle," *American Journal of Physiology-Heart and Circulatory Physiology*, vol. 286, 2004.
- [54] M. Drobna, A. Misak, T. Holland et al., "Captopril partially decreases the effect of H_2S on rat blood pressure and inhibits H_2S -induced nitric oxide release from S-nitrosoglutathione," *Physiological Research*, vol. 64, no. 4, pp. 479–486, 2015.
- [55] S. S. Franklin, S. A. Khan, N. D. Wong, M. G. Larson, and D. Levy, "Is pulse pressure useful in predicting risk for coronary heart disease?," *Circulation*, vol. 100, no. 4, pp. 354–360, 1999.
- [56] P. M. Mottram, B. A. Haluska, R. Leano, S. Carlier, C. Case, and T. H. Marwick, "Relation of arterial stiffness to diastolic dysfunction in hypertensive heart disease," *Heart*, vol. 91, no. 12, pp. 1551–1556, 2005.
- [57] N. Geoffroy and G. P. Demopoulos, "The elimination of selenium(IV) from aqueous solution by precipitation with sodium sulfide," *Journal of Hazardous Materials*, vol. 185, no. 1, pp. 148–154, 2011.
- [58] B. Jung, A. Safan, B. Batchelor, and A. Abdel-Wahab, "Spectroscopic study of Se(IV) removal from water by reductive precipitation using sulfide," *Chemosphere*, vol. 163, pp. 351–358, 2016.
- [59] M. Pettine, F. Gennari, L. Campanella, B. Casentini, and D. Marani, "The reduction of selenium(IV) by hydrogen sulfide in aqueous solutions," *Geochimica et Cosmochimica Acta*, vol. 83, pp. 37–47, 2012.
- [60] J. Hahn and R. Klüensch, "Synthesis and characterization of the first thiaselanes," *Angewandte Chemie International Edition in English*, vol. 33, no. 17, pp. 1770–1772, 1994.
- [61] M. Grman, M. Nasim, R. Leontiev et al., "Inorganic reactive sulfur-nitrogen species: intricate release mechanisms or cacophony in yellow, blue and red?," *Antioxidants*, vol. 6, no. 1, 2017.



Hindawi

Submit your manuscripts at
www.hindawi.com

